Optimal Filter Length and Zero Padding Length Design for Universal Filtered Multi-carrier (UFMC) System

Lei Zhang, Ayesha Ijaz, Pei Xiao, Kezhi Wang, Deli Qiao and Muhammad Ali Imran

***Abstract*—Universal filtered multi-carrier (UFMC) systems offer a flexibility of filtering arbitrary number of subcarriers to suppress out of band (OoB) emission, while keeping the orthogonality between subcarriers and robustness to transceiver imperfections. Such properties enable it as a promising candidate waveform for Internet of Things (IoT) communications. However, subband filtering may affect system performance and capacity in a number of ways. In this paper, we first propose the conditions for interference-free one-tap equalization and corresponding signal model in the frequency domain for UFMC system. The impact of subband filtering on the system performance is analyzed in terms of average signal-to-noise ratio (SNR), capacity and bit error rate (BER) and compared with the orthogonal frequency division multiplexing (OFDM) system. This is followed by filter length selection strategies to provide guidelines for system design. Next, by taking carrier frequency offset (CFO), timing offset (TO), insufficient guard interval between symbols and filter tail cutting (TC) into consideration, an analytical system model is established. In addition, a set of optimization criteria in terms of filter length and guard interval/filter TC length subject to various constraints is formulated to maximize the system capacity. Numerical results show that the analytical and corresponding optimal approaches match the simulation results, and the proposed equalization algorithms can significantly improve the BER performance.**

***Index Terms*—universal filtered multi-carrier, transceiver imperfection, zero padding, optimization, one-tap interference-free equalization, performance analysis. IoT**

I. Introduction

As a promising air-interface waveform candidate solution for the 5th generation wireless communications and beyond, universal filtered multi-carrier (UFMC) has drawn significant attentions by academia and industry in the last few years [1], [2], [3], [4], [5]. It inherits advantageous properties of OFDM systems, e.g., ease in the implementation of multi-antenna techniques low complexity and effective one-tap channel equalization [6], [7], but offers significantly lower out-of-band (OoB) emission than OFDM system [1], [2], [3], leading to improved spectrum efficiency. Comparing with filter-bank multi-carrier (FBMC) system [8], [9], UFMC system provides flexibility to filter a subband that consists of an arbitrary number of consecutive subcarriers, which provide a possibility of utilizing fragmented spectrum for short package communication, such as narrowband Internet of Things (NB-IoT). In addition, it has been reported in [10], [11] that UFMC system is more robust to transceiver imperfections such as carrier frequency offset (CFO) and timing offset (TO), which is a critical design criterion for a waveform when employed in multi-cell cooperation scenarios and low-cost low-complexity devices (e.g. machine type communications (MTC) and low-end IoT devices) [12]. In addition to the benefits in performance and the OoB emission, the most significant advantage of the UFMC system over OFDM system is the *design flexibility*, which enables the system to adapt to the requirements of specific user, service types and channels by adjusting the subband filter and system parameters.

All the benefits listed above are subject to proper subband filter design. For a given type of subband filter [1], the filter length is a key parameter affecting the system performance in different ways. A longer filter not only leads to lower OoB emission, but also results in better frequency localization and makes the system more robust to synchronization errors and multipath fading channels. However, a longer filter also causes several drawbacks including more frequency selective filter response (or narrower filter bandwidth) along subcarriers within one subband and larger overhead, reducing transmission efficiency in the time domain.

The effects on system performance are even more intricate when considering filter tail cutting (TC) to save overhead or insertion of guard interval between symbols to combat the effect of multipath fading channel. In the original UFMC implementation, guard interval between symbols such as cyclic prefix (CP) or zero padding (ZP) is not required in order to save the overhead [4], [13], [14], [15]. Such a system is not orthogonal in multipath fading channel environments and one-tap equalization is not interference-free. However, it has been claimed that the filter length takes approximately the same length as the CP length in an OFDM system, leading to negligible performance loss [4], [16], [10]. This is due to soft protection, against the multipath channel effect, provided by filter ramp up and ramp down at the edges of symbols. However, this claim has not been proved analytically and it does not hold in some scenarios such as harsh channel conditions, where the filter ramp up and ramp down at the

Lei Zhang and Muhammad Ali Imran are with School of Engineering, University of Glasgow, Glasgow, G12 8QQ, UK. Ayesha Ijaz is with NEC, Leatherhead, KT22 7SA, UK. Pei Xiao is with the 5G Innovation Centre (5GIC), University of Surrey, Guildford, GU2 7XH, UK. Kezhi Wang is with the University of Northumbria, Newcastle-upon-Tyne NE1 8ST, UK. Deli Qiao is with School of Information Science and Technology, East China Normal University, Shanghai, China. The work was supported in part by U.K. Engineering and Physical Sciences Research Council (EPSRC) under grants EP/S02476X/1 and EP/R001588/1.

[1]Note that the subband filter is a bandpass filter, and normally is symmetrical with well time and frequency localization property. In addition, Chebyshev filter is a favourable selection for UFMC system [2].

edges of symbols might not be sufficient to overcome the multipath channel and the performance loss is likely to be significant. Alternatively, cyclic prefix (CP) as an option can be added to avoid the inter-symbol interference (ISI) [2], [17]. However, the system can not achieve interference-free one-tap equalization either since the circular convolution property is destroyed. On the other hand, filter tail can be cut partly (preferably from both sides) to further reduce the system overhead as compared to the state-of-the-art (SoTA) UFMC system. This operation may result in performance loss but reduces the overall overhead. However, OoB emission level might be affected by the TC operation depending on the cutting length. In order to analyze the impact of filter length, ZP/CP or filter TC on the performance of a UFMC system and give useful guidelines for the system design, it is necessary to build a system model by taking all of the listed imperfection factors into consideration in multipath fading channel. A comprehensive analytical framework is also essential for optimal design of equalization and channel estimation algorithms.

Insufficient CP length with CFO and TO errors are modeled in [18] for OFDM systems and the optimal CP length for maximizing capacity is formulated in [19]. For the UFMC system, the original UFMC has been shown to be less susceptible to CFO and TO in comparison to CP-OFDM [4] via numerical results and simulations. For analytical model, the performance of UFMC systems in the presence of CFO was analyzed in [13] and a filter was optimized to minimize the out of band leakage (OBL) in [20] by considering both CFO and TO. However, only single-path flat fading channel was considered in [13] and [20]. In addition, the signal model in [20] is not fully derived as it contains convolution operation in the analytical expression. While such a model is important to evaluate a practical communication system, especially for systems which involves low cost and low complexity MTC/IoT devices.

Theoretically, to completely eliminate the effect of multipath channel by one-tap channel equalization, ZP/CP length longer or equal to the channel length should be added between UFMC symbols. However, similar to an OFDM system, sufficient ZP/CP length may yield marginal performance improvement at the cost of unnecessary overhead [19]. Moreover, in some scenarios (e.g., short channel length) ZP is not required at all, and the filter TC might be necessary to further reduce the system overhead. Therefore, for an optimal system, we conjecture that there is an optimal length of ZP/CP, filter TC and filter that is neither too short to combat the channel multipath effect, CFO and TO, nor too long to compromise the transmission efficiency. To the best of our knowledge, this is still an open issue for UFMC systems. The CP-UFMC system has been proposed in [17] and the performance are analyzed with insufficient CP length. In addition, a subband filtered multicarrier (SFMC) based multi-service system framework has been proposed in [21]. The system can flexibly support multiple types of services with each having its optimal frame structures and a low OoBE waveform (e.g., UFMC) working on the top to isolate the inter-service-band-interference. However, the properties of UFDM system and how does the filter parameters affect the single service band performance has not been investigated.

In this paper, we first consider an ideal case for MU-UFMC systems in Section II where the transceivers are assumed to be perfectly synchronized without any CFO and TO. Propositions are made for interference-free one-tap equalization, performance comparison to OFDM system and filter length selection. To reduce the overhead and adapt imperfect transceiver, the signal model for MU-UFMC considering insufficient ZP length, TC, CFO and TO is derived in Section III. In addition, new equalization algorithms are proposed to improve the system performance. Based on this analytical framework, a set of optimization problems in terms of filter length and ZP length is formulated to maximize the capacity in Section IV. The contributions and novelties of this paper are summarized as follows:

- In the absence of transceiver imperfections (e.g., CFO, TO, etc.), we first make propositions to illustrate the conditions for interference-free one-tap equalization and the corresponding system model for MU-UFMC system. Then a set of propositions is proposed and proved for performance analysis in terms of subband average output SNR, capacity per subcarrier and BER. These properties explain the performance loss due to introducing subband filtering in UFMC systems in ideal case in comparison to OFDM system. In addition, we define a new metric for UFMC subband filter, i.e., peak-to-bottom-power-ratio (PBPR) as a key parameter to guide the filter length selection.
- We derive an analytical expression for MU-UFMC system signal in terms of desired signal, inter-carrier interference (ICI), inter-symbol interference (ISI) and noise by considering insufficient ZP length, filter TC, CFO and TO. This analytical framework provides useful guidelines for practical algorithm design and further system performance analysis. The work also explains why the UFMC system is robust to dispersive channels and transceiver imperfections. In addition, it also calculates how much performance loss will be incurred in a given channel and transceiver imperfections.
- We propose a set of optimization criteria in terms of filter, ZP (or TC) length to maximize the system capacity. We start from a set of capacity optimization problems without the overhead constraint. This can be done e.g. by fixing filter length to optimize the ZP (or TC) length, or vice versa, or in a more general case, optimizing both filter length and ZP (or TC) length to achieve the global optimal solutions. On the other hand, when the system is designed with a fixed overhead, we optimize the proportion between filter length and ZP length to maximize the system capacity. The optimization problems represent different system design criteria to meet different design requirements in various environments.
- Based on the analytical framework, the derived signal model and variances of ICI and ISI, we propose a set of channel equalization algorithms, by considering not only the noise but also the interference, which can provide significant gain in terms of BER performance in

comparison to OFDM and the SoTA UFMC systems.

Notations: Vectors and matrices are denoted by lowercase and uppercase bold letters, and $\{\cdot\}^H, \{\cdot\}^T, \{\cdot\}^*$ stand for the Hermitian conjugate, transpose and conjugate operation, respectively. $\mathcal{E}\{a\}$ denotes the expectation of a. We use trace$\{\mathbf{A}\}$ to denote taking the trace of matrix $\mathbf{A}$. diag$\{\mathbf{a}\}$ refers to reframing a diagonal matrix with its diagonal elements being the elements of vector $\mathbf{a}$. $\mathbf{I}_M$ and $\mathbf{0}_{m\times n}$ refer to $M \times M$ identity matrix and $m \times n$ zero matrix, respectively. Operator $*$ denotes linear convolution of two vectors. $\lceil a \rceil$ and $\lfloor a \rfloor$ denote ceiling and floor operations on a, respectively.

II. MU-UFMC System Model and Performance Analysis in the Absence of Transceiver Imperfection

A. MU-UFMC System

Let us consider a multicarrier system with N subcarriers with the index set $\mathcal{U} = [0, 1, \cdots, N-1]$. The N subcarriers are divided into M subbands with the m-th subband comprising of N_m consecutive subcarriers from set $\mathcal{U}$ and $N_0+N_1+\cdots N_{M-1} = N$ [2]. It implies that the subcarrier index set for the m-th subband is $\mathcal{U}_m = [\sum_{i=0}^{m-1} N_i, \sum_{i=0}^{m-1} N_i + 1, \cdots, \sum_{i=0}^{m} N_i - 1]$. Note that the following derivations are for downlink transmission, however, the basic idea can be easily extended to uplink. In the MU scenario, we assume that the M subbands are assigned to K users each occupying from at least 1 to several subbands depending on system design and radio resource management. The subbands allocated to one user can be either contiguous or non-contiguous to achieve frequency diversity gain.

Assume the modulated symbols transmitted on the N subcarriers are $\mathbf{a} = [a(0), a(1), \cdots, a(N-1)]^T$ and $\mathcal{E}\{|a(i)|^2\} = \rho_{sym}^2$, for $i = 0, 1, \cdots, N-1$. Split the vector $\mathbf{a}$ into non-overlapping sub-vectors as $\mathbf{a} = [\mathbf{a}_0; \mathbf{a}_1; \cdots; \mathbf{a}_{M-1}]$, where $\mathbf{a}_m = [a(\sum_{i=0}^{m-1} N_i), a(\sum_{i=0}^{m-1} N_i+1), \cdots, a(\sum_{i=0}^{m} N_i-1)]^T$ is an N_m column vector consisting of symbols $a(i)$ transmitted in the m-th subband, as shown in Fig. 1. Let us assume that the m-th subband filter is $\mathbf{f}_m = [f_m(0), f_m(1), \cdots, f_m(L_{F,m}-1)]$ and without loss of generality, we assume that the power of $\mathbf{f}_m$ is normalized to unity, i.e., $\sum_{i=0}^{L_{F,m}-1} |f_m(i)|^2 = 1$. Generally, the filter lengths for different subbands (e.g., $L_{F,m1}$ and $L_{F,m2}$) are not necessarily the same, particularly for the subbands assigned to different users. For a unified expression for MU-UFMC, let us assume $L_{F,max} = max(L_{F,m})$ for $m \in [0, 1, \cdots, M-1]$ and define $\mathbf{A}_m \in \mathbb{C}^{(N+L_{F,max}-1)\times N}$ as the Toeplitz matrix of $\mathbf{f}_m$ with its first column being $\tilde{\mathbf{f}}_m = [\mathbf{f}_m, \mathbf{0}_{1\times(N+L_{F,max}-1-L_{F,m})}]^T \in \mathbb{C}^{(N+L_{F,max}-1)\times 1}$ and first row being $[f_m(0), \mathbf{0}_{1\times(N-1)}] \in \mathbb{C}^{1\times N}$. We can write the transmitted signal after subband filtering, as shown in Fig. 1, as:

$$\mathbf{q} = \sum_{m=0}^{M-1} \frac{1}{\rho_m} \mathbf{f}_m * (\mathbf{D}_m \mathbf{a}_m) = \sum_{m=0}^{M-1} \frac{1}{\rho_m} \mathbf{A}_m \mathbf{D}_m \mathbf{a}_m \ , \qquad (1)$$

[2]This equation implies that all of the N consecutive subcarriers are occupied. Otherwise, the transmitting symbols can be set to zero at the unoccupied subcarriers to satisfy the assumption.

where $\mathbf{D}_m \in \mathbb{C}^{N\times N_m}$ is the $(\sum_{i=0}^{m-1} N_i + 1)$-th to the $(\sum_{i=0}^{m} N_i)$-th columns of the N-point normalized IDFT (inverse discrete Fourier transform) matrix $\mathbf{D}$. The element of $\mathbf{D}$ in the i-th row and n-th column is $d_{i,n} = \frac{1}{\sqrt{N}} e^{j\cdot 2\pi i n/N}$. $\rho_m = \sqrt{\frac{1}{N_m} \text{trace}(\mathbf{D}_m^H \mathbf{A}_m^H \mathbf{A}_m \mathbf{D}_m)}$ is the transmission power normalization factor of the m-th subband. Due to the filter tail, $\mathbf{q}$ is $L_{F,max}-1$ samples longer than the original input signal $\mathbf{a}$.

Unlike the OFDM system that treats all subcarriers equally by a unified IDFT operation, equation (1) implies that UFMC implemented in Fig. 1 splits the whole bandwidth into subband and the signals transmitting in each subband $\mathbf{a}_m$ is operated by the IDFT and subband filter in series. Then the processed signals in all subbands $\frac{1}{\rho_m} \mathbf{A}_m \mathbf{D}_m \mathbf{a}_m$ are summed together for transmission to the receivers.

Two different operations can be performed before transmitting filtered signal to the users via wireless channel, as shown in Fig. 1. One can either insert CP/ZP between symbols to combat the effect of multipath channel fading or cut the filter tails from either sides of $\mathbf{q}$ in order to reduce overhead albeit at the expense of performance loss. The former may result in performance gain in harsh channel conditions but would incur additional overhead in the system in addition to filter tails. Note that ZP and CP insertions are equivalent to OFDM in terms of SNR performance in the ideal case [3] [24]. In this paper, we only consider zero padding and the model for CP insertion can be derived in a similar way. For brevity, in the rest of the paper, we will use OFDM to refer to ZP-OFDM, unless specified otherwise. On the other hand, the tail cutting operation saves the overhead but may result in performance loss due to the loss of the filter integrity. To unify the expression of ZP and filter TC scenarios and simplify the following derivations by a single parameter L_{ZP}, we define

$$\tilde{\mathbf{q}} = \begin{cases} [\mathbf{q}; \mathbf{0}_{L_{ZP}\times 1}] \in \mathbb{C}^{(N+L_{F,max}-1+L_{ZP})\times 1} & \text{if } L_{ZP} \geq 0 \\ \hat{\mathbf{q}} \in \mathbb{C}^{(N+L_{F,max}-1+L_{ZP})\times 1} & \text{if } L_{ZP} < 0 \end{cases} \qquad (2)$$

$\hat{\mathbf{q}}$ is the filter vector after tail cutting comprising of the $(\lfloor \frac{|L_{ZP}|}{2} \rfloor$+1)-th to the $(N + L_{F,max} - |L_{ZP}| + \lfloor \frac{|L_{ZP}|}{2} \rfloor - 1)$-th elements of $\mathbf{q}$. In other words, the front $\lfloor \frac{|L_{ZP}|}{2} \rfloor$ and the end $|L_{ZP}| - \lfloor \frac{|L_{ZP}|}{2} \rfloor$ elements of $\mathbf{q}$ are cut off to reduce overhead. Theoretically, the TC length $|L_{ZP}|$ should be less than $L_{F,max}-1$ to keep the length of $\hat{\mathbf{q}}$ equal to or larger than N. However, in most cases, for low level of OoB emission, we should keep the TC length much smaller than the filter length, i.e., $|L_{ZP}| << L_{F,max}$.

Equation (2) indicates that when $L_{ZP} \geq 0$, ZP will be performed on $\mathbf{q}$ before it is transmitted over the wireless channel, while filter TC will be performed on $\mathbf{q}$ when $L_{ZP} < 0$. However, whether $L_{ZP} \geq 0$ or $L_{ZP} < 0$, the UFMC symbol length will be $N + L_{F,max} + L_{ZP} - 1$ and the overhead is $L_{F,max} + L_{ZP} - 1$, which is attributed to both filter tails and ZP/TC.

Let us assume the channel between the transmitter and the k-th user at time t is $\mathbf{h}_k(t) = [h_k(0,t), h_k(1,t), \cdots, h_k(L_{CH,k} - 1, t)]$ where $L_{CH,k}$

[3]However, one should note that the CP and ZP OFDM systems can have different power spectrum density performance [22], [23].

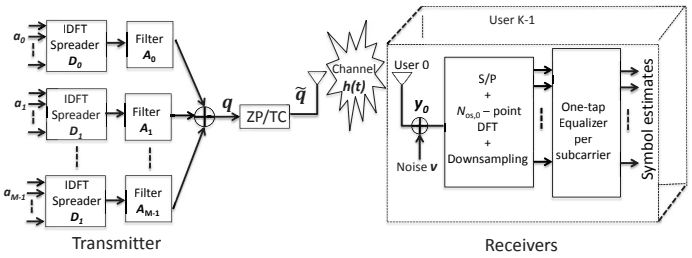

Fig. 1. Blocks diagrams for MU-UFMC transmitter and receiver.

is the length of the channel in UFMC samples. Without loss of generality, we assume the overall channel gain for the k-th user is $\sum_{i=0}^{L_{CH,k}-1} \mathcal{E}|h_k(i,t)|^2 = \rho_{CH,k}^2$. Using equation (1), the received signal at the k-th user can be written as:

$$\mathbf{y}_k = \mathbf{h}_k(t) * \tilde{\mathbf{q}} + \mathbf{v}_k = \mathbf{B}_k(t) \sum_{m=0}^{M-1} \mathbf{A}_m \mathbf{D}_m \mathbf{a}_m + \mathbf{y}_{k,ISI} + \mathbf{v}_k \ , \quad (3)$$

where $\mathbf{v}_k = [v_k(0), v_k(1), \cdots, v_k(N + L_{F,max} + L_{CH,k} - 2)]^T$ is a complex-valued noise vector for the k-th user and its elements are drawn from Gaussian distribution with zero mean and variance σ^2. $\mathbf{B}_k(t) \in \mathbb{C}^{(N+L_{F,max}+L_{CH,k}-2)\times(N+L_{F,max}-1)}$ is the equivalent channel convolution Toeplitz matrix of $\mathbf{h}_k(t)$. $\mathbf{y}_{k,ISI}$ is the ISI due to insufficient ZP length. In the ideal scenario without ISI, i.e., for $\mathbf{y}_{k,ISI} = \mathbf{0}$, the ZP length should satisfies $L_{ZP} \geq L_{CH,k} - 1$. This condition will be given and proved in Proposition 1 in the next subsection. However, the detailed expression for the ISI $\mathbf{y}_{k,ISI}$ will be given in Section III in the presence of synchronization errors and insufficient guard interval between symbols. When $L_{ZP} = 0$ and $K = 1$, the system model in (3) is equivalent to SoTA UFMC system [2], [4]. On the other hand, when $L_{F,m} = 1$, (3) is equivalent to an OFDM system.

We assume that the channel vector $\mathbf{h}_k(t)$ has the following property [6], [7]:

$$\mathcal{E}\{h_k(l_1,t_1)h_k^*(l_2,t_2)\} = \delta(l_1 - l_2)R_k(l_1, t_1 - t_2) \ , \quad (4)$$

where $R_k(l_1, t_1 - t_2)$ is the autocorrelation function of the channel $\mathbf{h}_k(t)$ at the l_1-th path and l_2-th path at time t_1 and t_2. $\delta(l)$ is the Kronecker delta function with $\delta(l) = 1$ for $l = 0$ and $\delta(l) = 0$ for $l \neq 0$. (4) implies that the channel taps are uncorrelated.

To simplify the derivation that follows, let us define:

$$\begin{aligned} L_1 &= N + L_{F,max} - 1, \quad L_{2,k} = L_1 + L_{CH,k} - 1, \\ L_3 &= N + L_{F,max} - 1 + L_{ZP} \ . \end{aligned} \quad (5)$$

B. Interference-free One-tap Equalization

To enable interference-free one-tap equalization design, it is very important to design a system wherein the frequency domain channel response and transmitted symbols have pointwise multiplicative relationship, or equivalently, circular convolution relationship in the time domain.

In the SoTA UFMC systems with N subcarriers, channel equalization is performed in several steps [2], [4]. First, $2N - L_{2,k}$ zeros are appended at the end of $\mathbf{y}_k$ to generate vector $\tilde{\mathbf{y}}_k$ with length $2N$. Then $2N$-point DFT is performed on $\tilde{\mathbf{y}}_k$, followed by down-sampling by a factor of 2. Finally, channel equalization is performed on the down-sampled signal. This implementation, however, will introduce ISI/ICI in one-tap channel equalization in two scenarios. First scenario is in multi-path fading channels where ISI will occur due to the lack of guard interval between symbols. Even with CP added [2], the original UFMC system cannot achieve interference-free one-tap equalization either since the circular convolution property is destroyed.

Secondly, the implementation of $2N$-point DFT operation implies that the filter length plus the channel length is smaller than N in order to make $2N - L_{2,k} \geq 0$. However, it is not necessary to limit the system design with this constraint in general.

To achieve interference-free one-tap equalization, we make the following proposition for the MU-UFMC system

Proposition 1: *Consider an MU-UFMC system that consists of N subcarriers allocated to K users with the transmitter and k-th user channel length being $L_{CH,k}$. Zero padding length at the transmitter (on $\mathbf{q}$ in equation (1)) is L_{ZP} and $N_{os,k}$-point DFT is performed at the receiver of the k-th user. A necessary and sufficient condition for interference-free one-tap channel/filter equalization at the receiver of the k-th user is:*

$$\begin{aligned} &L_{ZP} \geq L_{CH,k} - 1, \text{ and} \\ &N_{os,k} = 2^{\eta_k} N \text{ with } \eta_k \geq \lceil \log_2(\frac{L_{2,k}}{N}) \rceil \ , \end{aligned} \quad (6)$$

and the signal model for the n-th subcarrier of the k-th user in the m-th subband is

$$z_k(n) = \frac{1}{\rho_m \sqrt{2^{\eta_k}}} H_k(n,t) F_m(n) a(n) + v_{os,k}(n) \ , \quad (7)$$

where $v_{os,k}(n) = \sum_{l=0}^{L_{2,k}-1} \frac{1}{\sqrt{N_{os,k}}} e^{-j2\pi nl/N} v_k(l)$ is the noise after DFT and down-sampling operations. $H_k(n,t) = \sum_{l=0}^{L_{CH,k}-1} e^{-j2\pi nl/N} h_k(l,t)$ and $F_m(n) = \sum_{l=0}^{L_{F,m}-1} e^{-j2\pi nl/N} f_m(l)$ are the channel and filter response in *frequency domain*, respectively.

Proof: See Appendix A. ∎

From equation (7), it is obvious that the subcarriers are decoupled in frequency domain and the standard one-tap channel equalization algorithms such as ZF or MMSE can be applied. Note that $L_{CH,k}$ and $L_{F,m}$ could be larger than N. If $L_{CH,k} \leq N$ and $L_{F,m} \leq N$, then $H_k(n,t)$ and $F_m(n)$ are the n-th element of N-point DFT transformation of $\mathbf{h}_k(t)$ and $\mathbf{f}_m$, respectively. In any case, we have $\mathcal{E}|H_k(n,t)|^2 = \rho_{CH,k}^2$ and $\sum_{n=0}^{N-1} \mathcal{E}|F_m(n)|^2 = N_m \sum_{i=0}^{L_{F,m}-1} |f_m(i)|^2 = N_m$.

Proposition 1 gives conditions for interference-free equalization for user k in the MU-UFMC system. If we aim to achieve an interference-free system for all K users, the condition is specified as $L_{ZP} \geq L_{CH,max} - 1$ and $N_{os} = 2^{\eta_{max}} N$ with $\eta_{max} \geq \lceil \log_2(\frac{L_{2,max}}{N}) \rceil$, where $L_{2,max} = max(L_{2,k})$ for $k = 0, 1, \cdots, K-1$.

Proposition 2: *Consider an MU-UFMC system and the parameters setting for the k-th user satisfying Proposition 1.*

The SNR at the n-th subcarrier of user k in subband m can be written as:

$$\mathcal{E}\{SNR(n)\} = \frac{1}{\rho_m^2 2^{\eta_k}} \frac{\mathcal{E}|H_k(n,t)F_m(n)a(n)|^2}{\mathcal{E}|v_{os,k}(n)|^2} = \frac{N}{L_{2,k}} \cdot \frac{\rho_{sym}^2}{\sigma^2} \cdot \rho_{CH,k}^2 \cdot \frac{1}{\rho_m^2} \cdot |F_m(n)|^2 \quad (8)$$

Proof: Note that $\mathcal{E}|H_k(n,t)F_m(n)a(n)|^2 = \rho_{CH,k}^2 \rho_{sym}^2 |F_m(n)|^2$ since $\mathcal{E}|H_k(n,t)|^2 = \rho_{CH,k}^2$ and $\mathcal{E}|a(n)|^2 = \rho_{sym}^2$. Noise variance is given by $\mathcal{E}|v_{os,k}(n)|^2 = \mathcal{E}|\sum_{l=0}^{L_{2,k}-1} \frac{1}{\sqrt{N_{os,k}}} e^{-j2\pi nl/N} v_k(l)|^2 = \sum_{l=0}^{L_{2,k}-1} \frac{1}{N_{os,k}} \mathcal{E}|v_k(l)|^2 = L_{2,k}/N_{os,k}\sigma^2$. Substituting $N_{os,k} = 2^{\eta_k} N$ and expressions of signal and noise power into $\mathcal{E}\{SNR(n)\}$ leads to equation (8). ■

The SNR at the n-th subcarrier depends on the subband index m and the location of the subcarrier in the subband (i.e., index n), i.e., it is proportional to $\frac{1}{\rho_m^2}$ and $|F_m(n)|^2$. The latter in general is fixed but varies along the subcarriers in a particular subband. Fig. 2 gives an example of FIR Chebyshev filter response in frequency domain (i.e., $|F_m(n)|^2$) at different subcarriers. It clearly shows that the filter response depends on filter length and is frequency selective along subcarriers. It is also noted that the variance is considerably large when the filter length increases.

When filter length $L_{F,m} = 1$, equation (8) leads to an OFDM system with sufficient ZP length. Then $F_m(n)$ is constant along the subcarriers (as shown in Fig. 2) and $L_{2,k} = N + L_{CH,k} - 1$ with $L_{CH,k} - 1$ being the ZP length. We can easily obtain $\rho_m^2 = 1$, then signal model in (7) becomes $z(n) = \frac{1}{\sqrt{2^{\eta_k}}} H_k(n,t)a(n) + v_{os,k}(n)$. Consequently, (8) represents SNR for interference-free ZP-OFDM system as:

$$\mathcal{E}\{SNR^{ofdm}\} = \frac{N}{L_{2,k}} \cdot \frac{\rho_{sym}^2}{\sigma^2} \cdot \rho_{CH,k}^2 \quad \text{for} \quad n \in \mathcal{U} \,. \quad (9)$$

It can be concluded that UFMC is a generalized OFDM system. In addition, equation (9) confirms that the SNR of the n-th subcarrier is independent of its location in a subband and subband index itself. Therefore, the subband index m and subcarrier index n are omitted in the sequel.

C. Performance analysis and comparison with OFDM System

In comparison to OFDM system, Fig. 2 shows positive filter gain in the middle of a subband and negative filter gain at its edges. In order to present an overall view of the system performance in comparison to OFDM system *in perfect case (i.e., no CFO/TO/TC)*, we focus on the average performance in one subband, in terms of output SNR, capacity and BER. It is expecting that UFMC performs inferior than OFDM system with ideal transceivers. However, generic cases of UFMC system with transceiver imperfections will be discussed in Section III, where we will show the performance gain over the OFDM system.

1) Output SNR: The frequency selectivity of the filter is the essence of the UFMC system design to make the system well-localized in the frequency domain to combat multipath channel and reduce the OoB emission. However, similar to the side effects of the channel frequency selectivity, the filter frequency selectivity may cause system performance loss, as analyzed in the following proposition:

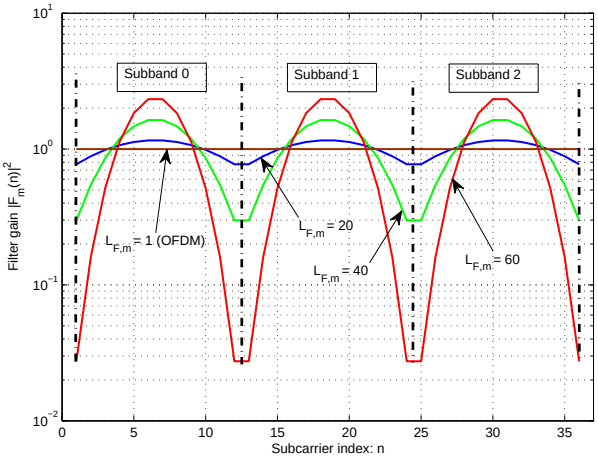

Fig. 2. Filter frequency response in 3 consecutive subbands for different filter length ($N = 240$, Chebyshev filter with OoB emission level -50 dB).

Proposition 3: *Consider an MU-UFMC system with $L_{F,m} > 1$ and the parameters for the k-th user satisfying equation (6) in Proposition 1. The subband filtering leads to performance loss in terms of average output SNR along the subcarriers in m-th subband in comparison to the OFDM system, i.e.,*

$$\mathcal{E}\{\overline{SNR}_m\} = \frac{1}{N_m} \sum_{n \in \mathcal{U}_m} \mathcal{E}\{SNR(n)\} \leq \mathcal{E}\{SNR^{ofdm}\} \,. \quad (10)$$

The equality holds only when $M = 1$.

Proof: See Appendix B. ■

This proposition implies that in the ideal case when equation (6) is satisfied, the UFMC system with only one subband will have the same performance as the OFDM system in terms of average SNR.

2) Capacity: The conclusion can be extended to system capacity without considering the overhead in high SNR region.

Proposition 4: *Consider an MU-UFMC system with $L_{F,m} > 1$ and assume the parameters for the k-th user satisfy equation (6) in Proposition 1. In addition, we assume the subband bandwidth is small enough to be within the coherence bandwidth. In the high-SNR region, i.e., $SNR(n) >> 1$, the MU-UFMC system incurs performance loss in terms of average capacity per subcarrier in the m-th subband in comparison to the OFDM system, i.e.,*

$$\overline{C}_m \approx \frac{1}{N_m} \mathcal{E}[\sum_{n \in \mathcal{U}_m} \log_2(SNR(n)] \leq C^{ofdm} \,. \quad (11)$$

The approximation leads to the relationship $\overline{C}_m = C^{ofdm} \approx \mathcal{E}(\log_2[\alpha/\rho_m^2 |H_k(i,t)|^2)$ with $\alpha = N/L_{2,k}\rho_{sym}^2/\sigma^2$ only when $M = 1$, i.e., the bandwidth has one subband only.

Proof: See Appendix C. ■

3) BER: Now we analyze the BER performance of quadrature amplitude modulation (QAM) schemes. The BER for M_{mod}-QAM can be calculated as [25]:

$$BER(n) = 2(1 - \frac{1}{\sqrt{M_{mod}}})Q\left(\sqrt{\frac{3SNR(n)}{M_{mod}-1}}\right). \quad (12)$$

The calculation of analytical BER expression is complex due to the Q-function $Q(\cdot)$. Thus, we use the following approximation of the Q-function as proposed in [25]:

$$Q(x) \approx \frac{1}{12}e^{-\frac{x^2}{2}} + \frac{1}{6}e^{-\frac{2x^2}{3}}. \quad (13)$$

Based on the approximation in (13), we have the following proposition:

Proposition 5: *Let us consider the same system as that assumed in Proposition 4. UFMC system in the m-th subband suffers performance loss in terms of average BER in the m-th subband as compared to the OFDM system, i.e.,*

$$\overline{BER}_m \geq BER^{ofdm}, \quad (14)$$

where $\overline{BER}_m = \frac{1}{N_m}\mathcal{E}\{\sum_{n\in\mathcal{U}_m} BER_m(n)\}$ and $BER^{ofdm} \approx \mathcal{E}(e^{-\phi_1|H_k(n,t)|^2\alpha} + e^{-\phi_2|H_k(n,t)|^2\alpha})$, with $\phi_1 = \frac{3}{2(M_{mod}-1)}$, $\phi_2 = \frac{2}{(M_{mod}-1)}$.

Proof: See Appendix D. ∎

Similarly, we have $\frac{1}{N_m}\sum_{n\in\mathcal{U}_m} e^{-\phi_2 SNR(n)} \geq e^{-\phi_2|H_k(i,t)|^2\alpha}$. Therefore, $\overline{BER}_m \geq \mathcal{E}(e^{-\phi_1|H_k(i,t)|^2\alpha} + e^{-\phi_2|H_k(i,t)|^2\alpha}) = BER^{ofdm}$.

Proposition 5 concludes that due to the introduction of the filter and unequal power allocation to different subcarriers, the average BER performance in one subband is worse than OFDM system. This is due to frequency selective filter response that is higher in the middle of the subband than the subcarriers at the edges. This leads to a high possibility of erroneous detection at the edges, while the response at middle subcarriers may be sometimes unnecessarily high leading to power waste.

D. Filter Length Selection

For a given type of filter, it is usually recommended that the filter length should be comparable to the channel length (or CP length in CP-OFDM systems), as proposed in the SoTA UFMC system [2], [4], [10], [16]. This claim is neither accurate nor generally applicable to all scenarios. As mentioned earlier, filter length impacts the performance in different ways. Without considering CFO, TO and insufficient ZP length, longer filter length leads to greater frequency selectivity and less effective power allocation along the subcarriers in a subband, resulting in performance loss.

To select a filter to achieve a given performance, we have to consider the performance in *every* subcarrier within the subband as proposed in Proposition 3, 4 and 5, which results in a very complex procedure.

To simplify the filter length selection procedure for a given performance, let us define a new metric: filter peak-to-bottom-gain-ratio (PBGR) in one subband as

$$\xi = \frac{|F_m(\lceil\frac{N_m}{2}\rceil)|^2}{|F_m(0)|^2}, \quad (15)$$

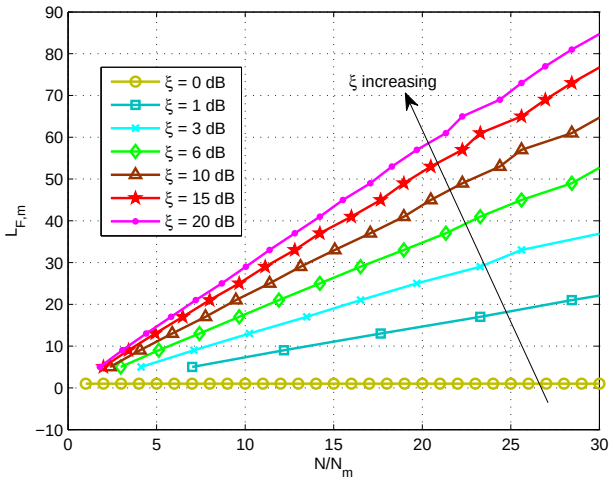

Fig. 3. Relation of filter length L_F with N/N_m in various PBGR ($N = 512$, Chebyshev-filter, OoB emission level -50 dB).

where $F_m(\lceil\frac{N_m}{2}\rceil)$ and $F_m(0)$ are filter frequency response at the middle and edge of the m-th subband, respectively. Instead of using filter response at all subcarriers in a subband, we exploit the single parameter ξ to map the subband performance approximately. To show the effectiveness of the simplification, we use numerical method to show the relationship of $L_{F,m}$ and N/N_m for different PBGR ξ in Fig. 3. The required filter length is increasing with N/N_m linearly. For example, if PBGR $\xi = 3$ dB and $N/N_m = 10$, (i.e., the whole bandwidth is 10 times of subband bandwidth) then from Fig. 3, we can see the filter length should be selected as 13. While $N/N_m = 20$, the filter length should be $L_{F,m} = 26$ approximately. Therefore, we have the following proposition.

Proposition 6: *The filter length $L_{F,m}$, parameter $\frac{N}{N_m}$ and PBGR ξ have the following linear relationship*

$$L_{F,m} = \lambda(\xi)\cdot\frac{N}{N_m}, \quad (16)$$

where $\lambda(\xi)$ is a non-zero scalar and it is a function of ξ. Unfortunately, $\lambda(\xi)$ can only be achieved by numerical method as in Fig. 3. We can also observe that smaller ξ leads to a more flat curve since it requires shorter filter to achieve a better PBGR (i.e., smaller ξ). $\xi = 0$ dB is an extreme case which refers to no frequency selectivity across the subcarriers in a subband and renders the UFMC system equivalent to an OFDM system (i.e., $L_{F,m} = 1$).

Proposition 6 (and Fig. 3) can be used in multiple ways for system design. For example, we can select appropriate subband bandwidth to achieve a certain ξ for a given total number of subcarriers N and filter length $L_{F,m}$. Similarly, for given filter length and N/N_m, it is easy to calculate corresponding ξ.

III. UFMC in the Presence of CFO, TO, TC and Insufficient ZP Length

In the previous section, we made some propositions on filter design and performance analysis of UFMC system in ideal cases, which sheds light on the system performance bound and

comparison to the OFDM system in ideal cases. However, due to the hardware impairments and imperfect synchronization mechanisms, a certain level of CFO and TO will always be present in practical systems. Moreover, sufficient ZP length is not always guaranteed (and sometimes unnecessary) in order to reduce the overhead of the system, and in some cases, the filter tail may be cut to further reduce the overhead. In this section, we will first derive the system model by taking all aforementioned imperfections into consideration. Based on this model, the performance is analyzed in terms of power of desired signal, ICI and ISI. Finally, new one-tap equalization algorithms are proposed.

In order to derive a unified expression for both TC and ZP on the filtered signal $\mathbf{q}$, we define the following parameter: let $L_{TC} = |L_{ZP}|$, $L_{TC,U} = \lfloor \frac{|L_{ZP}|}{2} \rfloor$ and $L_{TC,D} = |L_{ZP}| - L_{TC,U}$ if $L_{ZP} < 0$; $L_{TC} = L_{TC,U} = L_{TC,D} = 0$ if $L_{ZP} \geq 0$.

A. Signal model in the presence of CFO, TO and insufficient ZP length

Let us denote the CFO, normalized by subcarrier spacing Δf, in the m-th subband as ϵ_m[4]. Then we can rewrite the signal $\mathbf{q}$ in (1) as:

$$q(l) = \sum_{m=0}^{M-1} \sum_{i=0}^{N-1} \sum_{n \in \mathcal{U}_m} e^{j2\pi i(n+\epsilon_m)/N} f_m(l-i) a(n) \ , \quad (17)$$

where $l = L_{TC,U}, L_{TC,U}+1, \cdots, L_1 - 1 - L_{TC}$. Note here the range of l is such that both ZP and filter TC effects are taken into account. The first and the second summation are due to the filter response convolution and IDFT operations, respectively. The output of all filters at each subband will be added together and sent to the receiver over the channel. Considering τ_k as timing synchronization error, normalized by the sample duration ($\Delta T/N$ with ΔT being the symbol duration), at the k-th user, received signal at user k can be expressed as:

$$y_k(r) = \sum_{e=-\infty}^{\infty} \sum_{l=L_{TC,U}}^{L_1-1-L_{TC}} \sum_{m=0}^{M-1} \sum_{i=0}^{N-1} \sum_{n \in \mathcal{U}_m} e^{j2\pi i(n+\epsilon_m)/N} \cdot h_k(r-l-eL_3+\tau_k+L_{TC,U}, t) f_m(l-i) a(n) \ , \quad (18)$$

where $r = 0, 1, \cdots, L_3 - 1$. According to the Proposition 1, one of the conditions for k-th user to achieve the interference-free one-tap channel equalization is to set $L_{ZP} \geq L_{CH,k} - 1$. Therefore, $y_k(r) = 0$ for $r = L_3, L_3+1, \cdots, L_{2,k} - 1$. Generally, the selected ZP length is insufficient to reduce the overhead in the system. In other words, the non-zero $y(r)$ for $r = L_3, L_3+1, \cdots, L_{2,k}-1$ will overlap with the next UFMC symbol, causing ISI.

Let us assume $N_{os,k} = 2^{\eta_k} N$ point DFT is performed on $y_k(r,t)$ followed by down sampling by factor of η_k. Therefore,

[4]Generally, CFO is related to transmitter and receiver pair instead of subband directly. However, in order to simplify our derivation, we use ϵ_m, i.e., CFO for each subband. We can always set $\epsilon_{m_1} = \epsilon_{m_2}$ (for $m_1, m_2 \in [0, 1, \cdots, M-1]$) if both m_1-th and m_2-th subbands belong to the same user.

$$x_k(d) = \sum_{r=0}^{L_3} \sum_{e=-\infty}^{\infty} \sum_{l=L_{TC,U}}^{L_1-1-L_{TC}} \sum_{m=0}^{M-1} \sum_{i=0}^{N-1} \sum_{n \in \mathcal{U}_m} e^{\frac{j2\pi[i(n+\epsilon_m)-dr]}{N}} \cdot h_k(r-l-eL_3+\tau_k+L_{TC,U}, r-\tau_k) f_m(l-i) a(n) + v_{os,k}(d) \quad (19)$$

Equation (19) is a complete signal model taking the insufficient ZP, CFO and TO into consideration. $x_k(d)$ is a length N series and only $x_k(d)$ at d-th subcarrier that belongs to k-th user will be extracted for further symbol detection. In the next subsection, we will split (19) into three components, i.e., desired signal, ICI and ISI and express their powers for SINR and capacity calculation.

B. Performance analysis

Let us assume that the n-th subcarrier of the multicarrier symbol belongs to the k-th user and the m-th subband. The modulated symbols a_{n_1} and a_{n_2} are uncorrelated if $n_1 \neq n_2$ $\forall n_1, n_2 \in \mathcal{U}$. Moreover, since information symbols within different UFMC symbols are uncorrelated and $\mathcal{E}|a(n)|^2 = \rho_{sym}^2$, we can write the power of the signal received at the n-th subcarrier in terms of desired signal, ISI, ICI and noise as follows:

$$P_x(n) = P_D(n) + P_{ICI}(n) + P_{ISI}(n) + \frac{L_{2,k}}{N}\sigma^2 \ , \quad (20)$$

where

$$\begin{aligned} P_D(n) &= \rho_{sym}^2 \mathcal{E}|\beta(n,n,0)|^2 \ , \\ P_{ICI}(n) &= \rho_{sym}^2 \sum_{t \in \mathcal{U}_m, t \neq n} \mathcal{E}|\beta(n,t,0)|^2 \ , \\ P_{ISI}(n) &= \rho_{sym}^2 \sum_{e=-\infty, e\neq 0}^{\infty} \sum_{t \in \mathcal{U}_m} \mathcal{E}|\beta(n,t,e)|^2 \ , \end{aligned} \quad (21)$$

and $\beta(n,t,e)$ can be expressed as:

$$\beta(n,t,e) = \sum_{r=0}^{L_3} \sum_{l=L_{TC,U}}^{L_1-1-L_{TC}} \sum_{m=0}^{M-1} \sum_{i=0}^{N-1} e^{\frac{j2\pi[i(n+\epsilon_m)-rt]}{N}} h_k(r-l-eL_3+\tau_k+L_{TC,U}, r-\tau_k) f_m(l-i) \ . \quad (22)$$

To simplify the derivation of $|\beta(n,t,e)|^2$, let us define

$$T_m(l_1, l_2) = B_m(l_1) B_m^*(l_2) \ , \quad (23)$$

where $B_m(l_1) = \sum_{i=0}^{N-1} e^{\frac{j2\pi i(n+\epsilon_m)}{N}} f_m(l-i)$. Using (23), we have

$$\begin{aligned} \mathcal{E}|\beta(n,t,e)|^2 = & \sum_{l_1=L_{TC,U}}^{L_1-1-L_{TC}} \sum_{l_2=L_{TC,U}}^{l_1} \sum_{m=0}^{M-1} T_m(l_1,l_2) \sum_{r=l_1-l_2}^{L_3} \\ & e^{\frac{-j2\pi t(l_1-l_2)}{N}} R(r-l_1+\tau_k+L_{TC,U}, l_1-l_2) \\ & + \sum_{l_1=L_{TC,U}}^{L_1-1-L_{TC}} \sum_{l_2=l_1}^{L_1-1-L_{TC}} \sum_{m=0}^{M-1} T_m(l_1,l_2) \sum_{r=l_1-l_2}^{L_3-1-(l_2-l_1)} \\ & e^{\frac{-j2\pi t(l_1-l_2)}{N}} R(r-l_1+\tau_k+L_{TC,U}, l_1-l_2) \ . \end{aligned} \quad (24)$$

In the presence of interference, the SINR of the n-th subcarrier can be written as

$$SINR(n) = \frac{P_D(n)}{P_{ICI}(n) + P_{ISI}(n) + \sigma^2 L_{2,k}/N} \ . \quad (25)$$

Taking the overhead into consideration, the capacity of the whole bandwidth can be written as

$$C = \frac{N}{L_3} \sum_{n=0}^{N-1} \log_2[1 + SINR(n)] \ , \quad (26)$$

where $L_3 = N + L_{F,max} - 1 + L_{ZP}$ is the symbol length and $\frac{N}{L_3}$ is the spectrum efficiency factor.

C. Channel Equalization

Based on the derived signal model in the presence of receiver imperfections and insufficient ZP/TC length, the channel equalization algorithms can be updated accordingly. In this paper, two most widely used linear equalizers: ZF (zero-forcing) and MMSE (minimum mean square error) are considered. The equalizer for the n-th subcarrier can be expressed as

$$W_n = \frac{\beta(n,n,0)^H}{|\beta(n,n,0)|^2 + \nu\sigma_{eff}^2/\rho_{sym}^2} \ , \quad (27)$$

where ν is a parameter defined by

$$\nu = \begin{cases} 0 & \text{ZF receiver} \\ 1 & \text{MMSE receiver} \end{cases} \quad (28)$$

and

$$\sigma_{eff}^2 = P_{ISI} + P_{ICI} + \frac{L_{2,k}}{N}\sigma^2 \ , \quad (29)$$

where σ_{eff}^2 is the effective noise power taking ISI and ICI into consideration.

IV. Filter length and ZP length optimization

According to the capacity expression in (26) and the SINR in (25), the capacity of the UFMC system are affected by two adjustable factors, i.e., filter length and ZP/TC length, in an intricate manner. It is obvious from (26) that unnecessarily long filter length and ZP length/TC length is likely to lead to capacity reduction due to the overhead. On the other hand, too short ZP and filter length/TC length may also cause performance loss since system is not robust against the various imperfections and multipath fading channels. Next, we design the optimal UFMC system maximizing capacity subject to various constraints.

1) Optimal filter and ZP length without total overhead constraint: In the first instance, let us consider the case when filters in all subbands have the same length, i.e., $L_{F,0} = L_{F,1} = \cdots, L_{F,M-1} = L_{F,equal}$. By fixing the filter length $L_{F,m}$ to a constant value, we can formulate the following optimization problem in terms of ZP/TC length L_{ZP} to maximize system capacity:

$$\max_{L_{ZP}} C \quad \text{s.t.} \quad L_{F,equal} = \bar{L}_F \quad \text{and} \quad L_{ZP} \geq \bar{L}_{ZP} \ , \quad (30)$$

where $\bar{L}_F$ is a constant integer larger than zero. The second constraint is only required for TC case to avoid high level of OoB emission level. Unfortunately, the optimization problem can not be solved analytically due to the complex cost function. In the simulations, numerical methods will be adopted to solve (30).

On the other hand, we can optimize the filter length subject to a constraint on the ZP length:

$$\max_{L_{F,equal}} C \quad \text{s.t.} \quad L_{ZP} = \bar{L}_{ZP} \quad \text{and} \quad L_{F,equal} \geq \bar{L}_F \ . \quad (31)$$

The constraint $L_{F,equal} \geq \bar{L}_F > 0$ is added to meet the required OoB emission level. Again, $\bar{L}_{ZP}$ is a constant and it is not necessarily greater than zero.

Optimization problems in equation (30) and (31) are likely to yield local optimal values since both $L_{F,m}$ and L_{ZP} affect the performance and they are correlated. Therefore, we define the following generalized global optimization problem:

$$\max_{L_{ZP}, L_{F,equal}} C \quad \text{s.t.} \quad L_{F,equal} \geq \bar{L}_F \ . \quad (32)$$

Comparing to (30) and (31), (32) is an unconstrained optimization on either filter length or ZP length and, consequently leads to global optimization in terms of capacity.

2) Equal ZP and filter length for all subbands with overhead constraint: For a given system with fixed overhead budget (i.e., filter length plus ZP/TC length), selection of filter length and ZP length, such that their sum does not exceed the overhead budget, is another optimization problem of interest. For instance, reasonably longer filter length can improve the system frequency and time localization property and make it more robust to multipath fading channel, CFO and TO. However, it also implies a shorter ZP length and larger ISI may be caused in the multipath fading channel. Therefore, the capacity maximization optimization problem can be formulated as:

$$\max_{L_{ZP}, L_{F,equal}} C \quad \text{s.t.} \quad L_{F,equal} + L_{ZP} = \bar{L}_{OH} \quad \text{and} \quad L_{F,equal} \geq \bar{L}_F \ , \quad (33)$$

where $\bar{L}_{OH}$ is the system overhead that is equal to or larger than zero. Unlike (30), (31) and (32), where the overall overhead is not a constraint, the optimization in (33) can be conducted only by distributing the allocated overhead between filter length and ZP length. Therefore, optimization in (33) can not outperform (32). However, this optimization is suitable for the scenarios wherein the system is designed with fixed overhead.

3) Unequal ZP and filter length for all subbands with overhead constraint: In the multi-user case, it is reasonable to assume that each user experiences a different channel and has different receiver performance. Therefore, the optimization can be performed within each user subject to the equal symbol length (i.e., filter length plus ZP length for each user equals a constant). Then optimization (33) can be generalized as

$$\max_{\mathbf{L}_{ZP}, \mathbf{L}_F} C \quad \text{s.t.} \quad \mathbf{L}_F + \mathbf{L}_{ZP} = \bar{L}_{OH}\mathbf{1} \quad \text{and} \quad L_{F,m} \geq \bar{L}_F \quad \text{for} \quad m = 0, 1, \cdots, M-1 \ , \quad (34)$$

where $\mathbf{L}_{ZP} = [L_{ZP,0}, L_{ZP,1}, \cdots, L_{ZP,M-1}]$ and $\mathbf{L}_F = [L_{F,0}, L_{F,1}, \cdots, L_{F,M-1}]$. With different subband bandwidths, channel lengths or different receivers in MU case, (34)

gives more degree of freedom to adjust the parameters as compared to optimization in (33). This is likely to lead to better performance in versatile environments. However, the complexity of (34) is much higher than optimization problem (33) since the search space is $\bar{L}_{OH}^{M}$ instead of $\bar{L}_{OH}$ for (33).

V. Numerical results

In this section, we use Monte-Carlo simulations to compare the simulated and analytical results to verify the accuracy of derived signal models in (20) and the proposed propositions. In addition, the optimization problems proposed in (30), (31), (32) and (33) will be examined in various channels and transceiver imperfections. Finally, we will verify the proposed equalization algorithms in (27) and compare with OFDM and SoTA UFMC systems in terms of BER.

We adopt the 3rd Generation Partnership Project (3GPP) Long Term Evolution (LTE)/LTE-A defined radio frame structure, i.e., the whole bandwidth consists of 1200 subcarriers with subcarrier spacing $\Delta f = 15$ KHz and the symbol duration $\Delta T = 1/\Delta f = 1/15000$ s. In order to demonstrate the results clearly and without loss of generality, we consider that the middle $N = 36$ subcarriers have been divided into $M = 3$ equal bandwidth subbands occupied by $K = 3$ users, i.e., $N_i = 12$ for $i = 0, 1, 2$. Simulations are performed in three 3GPP specified channel models, i.e., Extended Pedestrian-A (EPA), Extended Vehicular-A (EVA) and Extended Typical Urban (ETU) [6] as well as International Telecommunication Union (ITU) specified channel model for Hilly Terrain (HT). We assume that the channel is static between the adjacent symbols. The signal is modulated using 16-QAM with normalized power and the input SNR is controlled by the noise variance. We adopt FIR Chebyshev filter [2] with 50 dB side lobe attenuation. For fair comparison, we assume the ZP length for OFDM system is the same as the total overhead for UFMC system (i.e., $L_{F,max} - 1 + L_{ZP}$). We also provide the results of ideal case (i.e., no CFO, TO and sufficient ZP length) for both UFMC and OFDM systems as benchmarks.

A. Signal model verification

To investigate the effect of CTO, TO and insufficient ZP length on system performance in terms of desired signal power, ICI power and ISI power, we consider the channels for the three users are EVA, ETU and EPA, respectively. The filter length $L_{F,equal} = 128$ and ZP length $L_{ZP} = 16$ for UFMC systems. The receivers of the three users are assumed to have different values of CFO and TO, with $\boldsymbol{\epsilon} = [\epsilon_0, \epsilon_1, \epsilon_2] = [0.06, 0.15, 0.04]$ and $\boldsymbol{\tau} = [\tau_0, \tau_1, \tau_2] = [160, 256, 80]$ samples which correspond to $0.078, 0.125, 0.039$ of LTE/LTE-A symbol duration.

Analytical results for desired signal $P_D(n)$ derived in equation (21) are compared with simulation results and shown in Fig. 4, where all of the analytical results match the simulation results, which shows the effectiveness and accuracy of the derived signal models. In both ideal and non-ideal cases, the UFMC system shows frequency selectivity over each subband, while the OFDM system shows equal response at different subcarriers. It also verifies the Proposition 2 in Section II

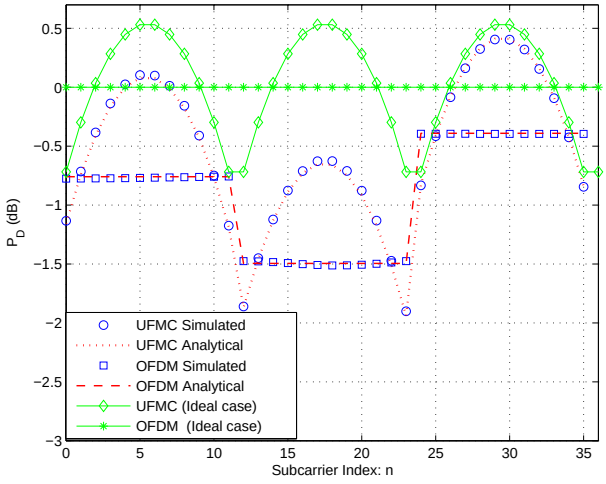

Fig. 4. Desired signal power versus subcarrier index for both ideal and interference cases.

that the middle subcarriers of each subband in UFMC system experience higher gain than the same subcarrier in an OFDM system. Whereas, at the edge of each subband, the UFMC system suffers power loss as compared to the OFDM system both in ideal and interference cases.

The analytical results for ICI and ISI power in equation (21) and simulation results for both UFMC and OFDM systems are shown in Fig. 5. Again, the simulation results match analytical results for all cases. Due to the subband filtering, the UFMC system shows frequency selectivity along subcarrier in each subband. However, the UFMC system suppresses the interference to a much lower level than the OFDM system in all subcarriers, especially for those (the last one) with small error. It is also observed from these results that for the three subbands with different receiver error, the UFMC system shows better error isolation property than the OFDM system. Specifically, the last subband (subcarrier index from 24 to 35) has much lower CFO and TO than the adjacent subbands, as shown in the figure where the third subband suffers from much lower ICI and ISI than the first two subbands. However, for the OFDM system, the results show that the third subband has only limited interference power reduction and prove that error propagation occurs among subcarriers.

The analytical (in equation (22)) and simulated output SINR for both UFMC and OFDM systems are shown in Fig. 6 for input SNR = 15 dB (i.e., $\sigma^2 = -15$ dB). It is observed that UFMC exhibits large SINR variation along the subcarriers in each subband in the error free case, while OFDM system shows a relatively flat line in ideal case. However, this is changed due to receiver errors and insufficient ZP, as we can see that UFMC outperforms OFDM system for each subcarrier even for subcarriers at the edge of subbands. This verifies that in the presence of insufficient ZP length and/or transceiver imperfections, the subband filter in UFMC system can improve the performance as compared to OFDM system.

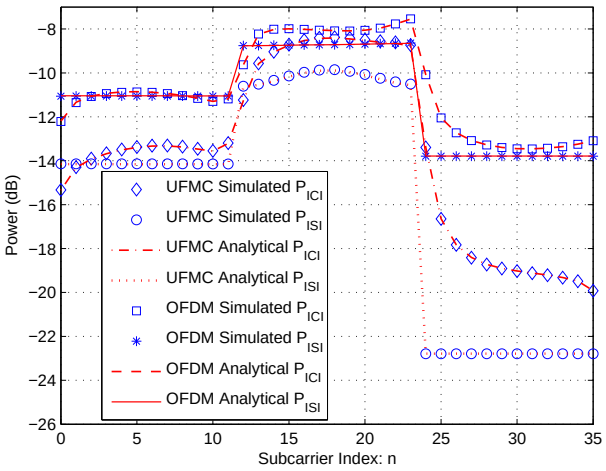

Fig. 5. ICI and ISI power versus subcarrier index for both ideal and interference cases.

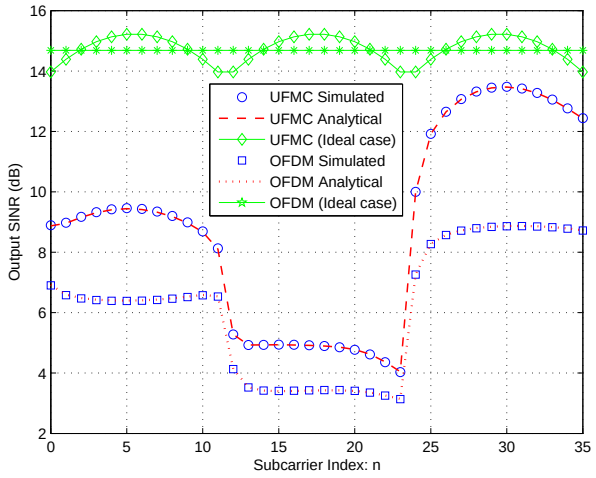

Fig. 6. Output SINR versus subcarrier index for both ideal and interference cases.

B. Optimizations

Next, we examine the optimization problems formulated in (30), (31), (32) and (33) by comparing with the simulation results considering various parameters. To simplify the analysis, we will use the same channel (ETU channel for all cases) and values of CFO and TO for all of the three users. Unless specified otherwise, all of the parameters remain the same as in the previous simulation in Section V-A.

Let us first consider the optimization (31) with fixed ZP length $\bar{L}_{ZP} = 0$. In order to show the impact of filter length on the system performance and the optimal solutions and its relationship with the error level, the capacity is plotted versus the filter length for different values of $\boldsymbol{\epsilon}$ and $\boldsymbol{\tau}$ in the left hand side subplot in Fig. 7. It can be seen from these results that the simulated and analytical curves overlap for all values of CFO and TO under study. Moreover, increasing values of CFO and TO increase the optimal filter length $L_{F,m}$. This implies that longer filter is required to combat larger receiver imperfections. Although longer filter can reduce the capacity degradation caused by larger CFO and TO, however, the peak values decrease with increased synchronization errors. In the absence of CFO and TO ($\boldsymbol{\epsilon} = \mathbf{0}$ and $\boldsymbol{\tau} = \mathbf{0}$), the capacity reduces worse than linear with increasing filter length due to both filter tail induced overhead and performance loss caused by frequency selective filter response.

By fixing the filter length $\bar{L}_F = 196$, capacity is shown in the right hand side subplot of Fig. 7 as a function of the ZP/TC length L_{ZP} for different channels. Note that $L_{ZP} > 0$ and $L_{ZP} < 0$ for the x-axis correspond to ZP and TC cases, respectively. The optimal ZP length for both LTE EPA and ETU channels is zero, i.e., neither ZP nor TC is required. However, the optimal ZP length is around 300 samples to combat the multipath fading channel in HT channel. In addition, the larger delay spread in HT channel leads to a much smaller maximum optimal capacity. The optimal capacity achieved in ETU channel is slightly larger than capacity in EPA channel. This is due to the reason that ETU channel is more frequency selective than EPA channel, which may result in a high possibility to have significantly larger SINR in some subcarriers than EPA channel. According to the system capacity calculation method in (26), the SINR in these subcarriers can increase $\sum_{n=0}^{N-1} \log_2[1+SINR(n)]$, also notice that they have the same optimal overhead $\frac{N}{L_3}$, which leads to the ETU channel outperforming EPA channel.

To study the global optimal filter length and ZP length, we plot 3D results in Fig. 8 by varying both L_F and L_{ZP}. To avoid confusion, only the analytical result is given. From the results, we verify the proposed optimization problem formulated in (33), i.e., selecting ZP and filter length for a fixed overhead budget to achieve the optimal capacity.

From Fig. 9 we can see the simulation and analytical results closely match for all four values of overhead under consideration. The capacity versus filter length behavior differs for different overhead budget $\bar{L}_{OH}$. For lower overhead $\bar{L}_{OH} = 80$, maximum capacity is achieved when all of the budget is used to accommodate a long filter length and there is no ZP at all. For larger overhead limit (from $\bar{L}_{OH} = 176$ to $\bar{L}_{OH} = 336$), the optimal filter length is fixed, which means that the total overhead proportion for filter is decreased. However, the maximum value decreases due to two reasons: a), long overhead leads to reduced capacity; b), from the perspective of output SINR performance, too long overhead can also cause performance loss since the noise error level linearly increases as the ZP length increases.

C. New channel equalization algorithms

Finally, we examine the effectiveness of the proposed equalization algorithm given in equation (27) in the presence of CFO, TO and insufficient ZP/TC length. The results are compared with the OFDM system, original UFMC system and the ideal case serving as benchmarks. The original UFMC system refers to the one that adopts the same channel equalization algorithm (e.g., MMSE) without considering the synchronization errors based on equation (7). Note that the MMSE

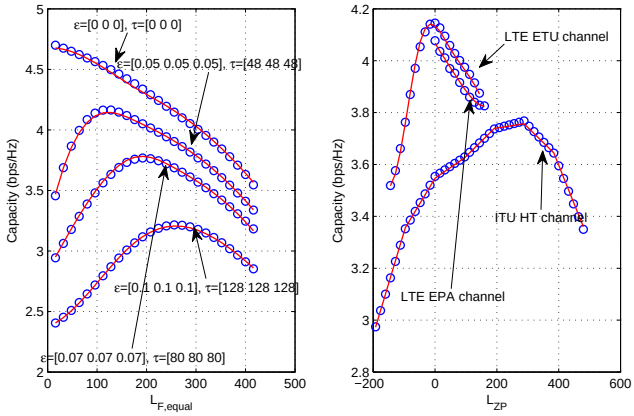

Fig. 7. System capacity versus filter length and ZP length (circles: simulated results; lines: analytical results), left: capacity versus filter length; right: capacity versus ZP/TC length.

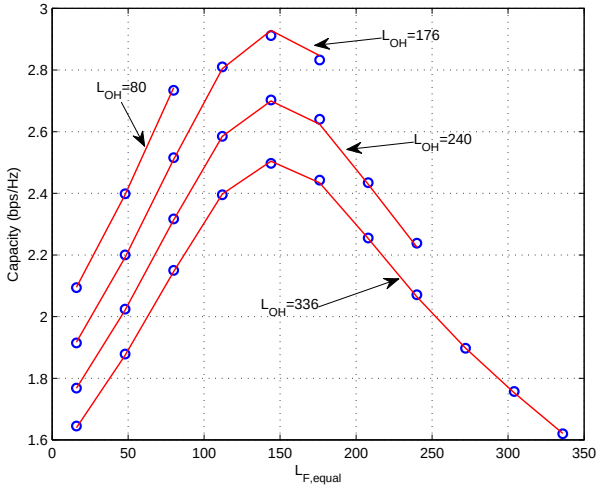

Fig. 9. System capacity versus filter length $L_{F,equal}$ for fixed overhead $\bar{L}_{OH}$ (circles: simulated results; lines: analytical results).

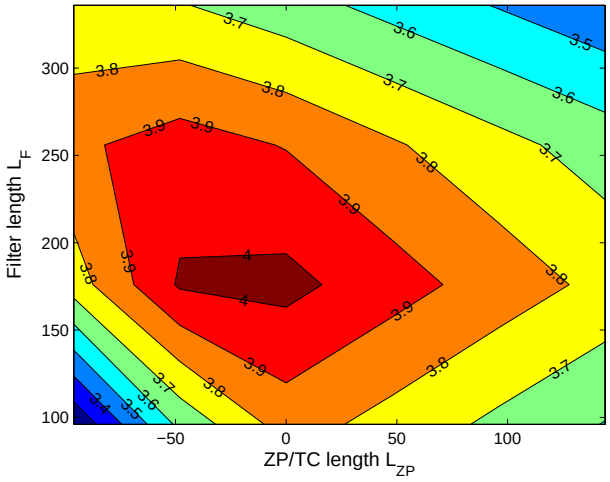

Fig. 8. System capacity (bps/Hz) versus filter length $L_{F,m}$ and ZP length L_{ZP}.

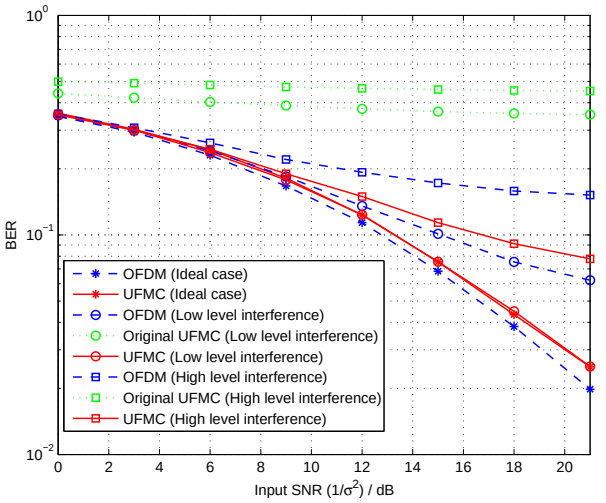

Fig. 10. BER performance versus input SNR.

and ZF equalizers show similar trend, we only present results for the MMSE-based algorithm. Simulations were performed using HT channel and two sets of interference parameters: the first set refers to the lower values of interference with $\boldsymbol{\epsilon}_L = [0.01, 0.03, 0.02]$; $\boldsymbol{\tau}_L = [16, 32, 16]$ and $L_{ZP} = 48$, while the second set refers to higher interference values as $\boldsymbol{\epsilon}_H = [0.05, 0.1, 0.1]$; $\boldsymbol{\tau}_H = [32, 64, 48]$ and $L_{ZP} = 144$. The filter length is fixed, i.e., $L_{F,m} = 64$ for all cases. Comparing the OFDM with UFMC system in ideal cases, it is seen in Fig. 10 that OFDM slightly outperforms UFMC system, thus verifying the Proposition 5 in Section II-C. However, in the presence of insufficient ZP, CFO and TO, the UFMC system shows its advantage over the OFDM system by suppressing errors effectively. This is consistent with our analysis and the simulation results shown in the previous subsections. For smaller synchronization errors, the UFMC system can achieve nearly the same performance as the ideal case, while the OFDM system suffers a significant performance loss. Larger synchronization errors cause performance loss in the UFMC system, however, compared with the OFDM system, UFMC can still achieve considerable gain.

VI. Conclusions

The MU-UFMC system has been modeled and analyzed with perfect receiver and sufficient ZP length between symbols in the work. Several propositions and system properties including the conditions for interference-free one-tap equalization and performance in comparison to OFDM system have been proposed in this paper. We proved analytically the reasons of performance loss in the UFMC system in terms of subband average SNR, capacity per subcarrier and BER in comparison to the OFDM system in ideal case. The model is extended to the scenarios of transceiver errors and insufficient ZP length/TC,

where the analytical power for desired signal, ICI and ISI are derived and a new set of equalization algorithms is proposed by taking these error factors into consideration. Based on this analytical framework, we proposed a set of criteria to optimize filter length and ZP/TC length subject to various constraints to maximize the system capacity. Our theoretical analysis and optimization problems have been validated via extensive simulations and analysis. The analytical framework developed in this paper reveals in-depth insights into the system behavior under different conditions and provides a valuable reference for the design and development of practical UFMC systems.

ACKNOWLEDGEMENT

The authors would like to acknowledge the support of the University of Surrey 5GIC (http://www.surrey.ac.uk/5gic) members for this work.

APPENDIX A
PROOF OF PROPOSITION 1

Obviously, to achieve ISI-free transmission ($\mathbf{y}_{k,ISI} = \mathbf{0}$) for the k-th user, zero padding length should satisfy $L_{ZP} \geq L_{CH,k} - 1$, i.e., the current symbol can not overlap the next in multi-path channel environments. Next, we focus on the conditions of achieving ICI-free one-tap equalization.

Let us pad $N_{os,k} - L_{2,k}$ zeros at the end of $\mathbf{y}_k$ to yield $\tilde{\mathbf{y}}_k = [\mathbf{y}_k; \mathbf{0}_{(N_{os,k}-L_{2,k})\times 1}] \in \mathbb{C}^{N_{os,k}\times 1}$. Assume $\mathbf{D}^H_{N_{os,k}}$ is the normalized $N_{os,k} \times N_{os,k}$ DFT matrix with $\mathbf{D}^H_{N_{os,k}}\mathbf{D}_{N_{os,k}} = \mathbf{I}_{N_{os,k}}$. Applying $N_{os,k}$-point DFT to $\tilde{\mathbf{y}}_k$ can be equivalently written as:

$$\tilde{\mathbf{z}}_k = \mathbf{D}^H_{N_{os,k}}\tilde{\mathbf{y}}_k = \mathbf{D}^H_{N_{os,k}}(\tilde{\mathbf{B}}_k(t)\sum_{m=0}^{M-1}\mathbf{A}_m\mathbf{D}_m\mathbf{a}_m + \tilde{\mathbf{v}}_k)\ , \quad (35)$$

where $\tilde{\mathbf{B}}_k(t) = [\mathbf{B}_k(t); \mathbf{0}_{(N_{os,k}-L_{2,k})\times(N+L_{max,F}-1)}]$ and $\tilde{\mathbf{v}}_k = [\mathbf{v}; \mathbf{0}_{(N_{os,k}-L_{2,k})\times 1}]$, respectively. Equation (35) can be reformulated as $\tilde{\mathbf{z}}_k = \mathbf{D}^H_{N_{os,k}}(\bar{\mathbf{B}}_k(t)\sum_{m=0}^{M-1}\bar{\mathbf{A}}_m\tilde{\mathbf{D}}_m\mathbf{a}_m + \tilde{\mathbf{v}})$, where $\tilde{\mathbf{D}}_m = [\mathbf{D}_m; \mathbf{0}_{N_{(os,k}-N)\times N}]$ and $\bar{\mathbf{B}}_k(t)$ is the circulant matrix of channel with the first column being $\bar{\mathbf{h}}_k(t) = [\mathbf{h}_k(t); \mathbf{0}_{(N_{os,k}-L_{CH,k})\times 1}]$ and $\bar{\mathbf{A}}_m$ is the circulant matrix of filter at the m-th subband with the first column being $\bar{\mathbf{f}}_m = [\mathbf{f}_m; \mathbf{0}_{(N_{os,k}-L_{F,m})\times 1}]$. Since $\mathbf{D}^H_{N_{os,k}}\mathbf{D}_{N_{os,k}} = \mathbf{I}_{N_{os,k}}$, we have

$$\begin{aligned}\tilde{\mathbf{z}}_k = \mathbf{D}^H_{N_{os,k}}\bar{\mathbf{B}}_k(t)\mathbf{D}_{N_{os,k}}\sum\nolimits_{m=0}^{M-1}\mathbf{D}^H_{N_{os,k}}\bar{\mathbf{A}}_m \\ \cdot\mathbf{D}_{N_{os,k}}\mathbf{D}^H_{N_{os,k}}\tilde{\mathbf{D}}_m\mathbf{a}_m + \mathbf{D}_{N_{os,k}}\tilde{\mathbf{v}}_k\ . \quad (36)\end{aligned}$$

Using the circular convolution property of $\bar{\mathbf{B}}_k(t)$ and $\bar{\mathbf{A}}_m$,

$$\begin{aligned}\mathbf{D}^H_{N_{os,k}}\bar{\mathbf{B}}_k(t)\mathbf{D}_{N_{os,k}} &= \sqrt{N_{os,k}}\text{diag}[\mathbf{D}_{N_{os,k}}\bar{\mathbf{h}}_k(t)] = \mathbf{H}_{N_{os,k}}(t) \\ \mathbf{D}^H_{N_{os,k}}\bar{\mathbf{A}}_m\mathbf{D}_{N_{os,k}} &= \sqrt{N_{os,k}}\text{diag}(\mathbf{D}_{N_{os,k}}\bar{\mathbf{f}}_m) = \mathbf{F}_{N_{os,k},m}\ , \quad (37)\end{aligned}$$

where $\mathbf{H}_{N_{os,k}}(t)$ and $\mathbf{F}_{N_{os,k},m}$ are diagonal matrices comprising of the frequency domain response of channel and filter, respectively. The n-th diagonal element of $\mathbf{H}_{N_{os,k}}(t)$ and $\mathbf{F}_{N_{os,k},m}$ can be written as $H_k(n,t) = \sum_{l=0}^{L_{CH,k}-1} e^{-j2\pi nl/N_{os,k}}h_k(l,t)$ and $F_m(n) = \sum_{l=0}^{L_{F,m}-1} e^{-j2\pi nl/N_{os,k}}f_m(l)$.

Substituting (37) in (36), and down sampling $\tilde{\mathbf{z}}_k$ by a factor of η_k, we have

$$\begin{aligned}(\tilde{\mathbf{z}}_k)^{\downarrow\eta_k} = \sum_{m=0}^{M-1}(\mathbf{H}_{N_{os,k}})^{\downarrow\eta_k}(\mathbf{F}_{N_{os,k},m})^{\downarrow\eta_k}(\mathbf{D}^H_{N_{os,k}}\tilde{\mathbf{D}}_m)^{\downarrow\eta_k}\mathbf{a}_m \\ +(\mathbf{D}_{N_{os,k}}\tilde{\mathbf{v}}_k)^{\downarrow\eta_k}\ , \quad (38)\end{aligned}$$

where both $(\mathbf{H}_{N_{os,k}})^{\downarrow\eta_k}$ and $(\mathbf{F}_{N_{os,k},m})^{\downarrow\eta_k}$ are diagonal matrices. To achieve the ICI-free one-tap equalization, $(\mathbf{D}^H_{N_{os,k}}\tilde{\mathbf{D}}_m)^{\downarrow\eta_k}$ should be a non-zero diagonal matrix. The i-th column and m-th row element of $(\mathbf{D}^H_{N_{os,k}}\tilde{\mathbf{D}}_m)^{\downarrow\eta_k}$ can be written as $\tilde{d}(i,m) = \sum_{l=0}^{N} e^{-j2\pi\eta_k il/N_{os,k}}e^{j2\eta_k in/N}$. To make the matrix non-zero diagonal, $(\mathbf{D}^H_{N_{os,k}})^{\downarrow\eta_k}$ and $\tilde{\mathbf{D}}_m$ should be taking from the orthogonal basic, and it holds true only if $N_{os,k}$ is an even multiple of N, i.e., $N_{os,k} = 2^{\eta_k}N$, $\eta_k \in \mathbb{R}^+$, and in this case $(\mathbf{D}^H_{N_{os,k}}\tilde{\mathbf{D}}_m)^{\downarrow\eta_k} = \frac{1}{\sqrt{2^{\eta_k}}}\mathbf{I}$. Combining with the inequality $N_{os,k} \geq L_{2,k}$, we have $\eta_k \geq \lceil\log_2(\frac{L_{2,k}}{N})\rceil$. For the noise, the n-th element of $(\mathbf{D}_{N_{os,k}}\tilde{\mathbf{v}})^{\downarrow\eta_k}$ can be expressed as $v_{os,k}(n) = \sum_{l=0}^{L_{2,k}}\frac{1}{\sqrt{N_{os,k}}}e^{-j2\pi nl/N}v_k(l)$. The n-th diagonal element of $(\mathbf{H}_{N_{os,k}})^{\downarrow\eta_k}$ and $(\mathbf{F}_{N_{os,k},m})^{\downarrow\eta_k}$ can be written as $H_k(n,t) = \sum_{l=0}^{L_{CH,k}} e^{-j2\pi nl/N}h_k(l,t)$ and $F_m(n) = \sum_{l=0}^{L_{F,m}} e^{-j2\pi nl/N}f_m(l)$. Substitute into (38), we obtain $z(n)$ as given in (7), where $\frac{1}{\rho_m\sqrt{2^{\eta_k}}}H_k(n,t)F_m(n)$ and $v_{os,k}(n)$ are scalar coefficients and processed noise. Both are independent of the modulated symbols $a(n)$ for $n \in U_m$. Thus, interference-free one-tap equalization can be performed.

APPENDIX B
PROOF OF PROPOSITION 3

For normalized filter in the m-th subband, we have $|F_m(0)|^2 + |F_m(1)|^2 + \cdots + |F_m(L_{F,m}-1)|^2 = N_m$. Using (8), we obtain $\overline{SNR}_m = \frac{1}{N_m}\mathcal{E}\{\sum_{n\in\mathcal{U}_m}SNR(n)\} = \frac{1}{N_m}\frac{N}{L_{2,k}\rho_m^2}\rho^2_{CH,k}\cdot\frac{\rho^2_{sym}}{\sigma^2}\sum_{n\in\mathcal{U}_m}|F_m(n)|^2 = \frac{N}{L_{2,k}\rho_m^2}\rho^2_{CH,k}\cdot\frac{\rho^2_{sym}}{\sigma^2}$. Whereas, the SNR for OFDM system is independent of the subcarrier index and is determined as $\overline{SNR^{ofdm}} = \frac{N}{L_{2,k}}\rho^2_{CH,k}\cdot\frac{\rho^2_{sym}}{\sigma^2}$.

Comparing SNR expression of UFMC to OFDM, the only difference is the normalization factor $\rho_m^2 = \frac{1}{N_m}\text{trace}(\mathbf{D}_m^H\mathbf{A}_m^H\mathbf{A}_m\mathbf{D}_m)$. To prove the performance loss, let us first define $\rho_B^2 = \frac{1}{N_m}\text{trace}(\mathbf{D}^H\mathbf{A}_m^H\mathbf{A}_m\mathbf{D}) = \frac{1}{N_m}\text{trace}(\mathbf{A}_m\mathbf{A}_m^H) = \frac{N}{N_m}$ with $\mathbf{D}$ being normalized N-point DFT matrix. ρ_B^2 can be also defined as $\rho_B^2 = \sum_{i=0}^{N-1}\frac{1}{N_m}\text{trace}(\mathbf{A}_m\mathbf{d}_i\mathbf{d}_i^H\mathbf{A}_m^H)$ with $\mathbf{d}_i$ being the i-th column of $\mathbf{D}$. Then $\rho_B^2 = \frac{1}{N_m}\sum_{i=1}^{N}\text{trace}(\mathbf{D}^H_{N_{os,k}}\bar{\mathbf{A}}_m\mathbf{D}_{N_{os,k}}\mathbf{D}^H_{N_{os,k}}\mathbf{d}_i\mathbf{d}_i^H\mathbf{D}_{N_{os,k}}\mathbf{D}^H_{N_{os,k}}\bar{\mathbf{A}}_m^H\mathbf{D}_{N_{os,k}}) = \frac{1}{N_m}\text{trace}(|(\mathbf{F}_{N_{os,k},m})|^2\tilde{\tilde{\mathbf{D}}}_i) = \frac{1}{N_m}|(\mathbf{F}_{N_{os,k},m})|^2\text{diag}[\tilde{\tilde{\mathbf{D}}}_i]$ with $\tilde{\tilde{\mathbf{D}}}_i = \mathbf{D}^H_{N_{os,k}}\tilde{\mathbf{d}}_i^H\tilde{\mathbf{d}}_i\mathbf{D}_{N_{os,k}}$. To simplify the analysis, let us define the i-th diagonal elements of $\tilde{\tilde{\mathbf{D}}}_i$ as $\tilde{\tilde{d}}_i(l)$, then $\rho_B^2 = \frac{1}{N_m}\sum_{l=0}^{N_{os,k}-1}|F_m(l)|^2\tilde{\tilde{d}}_i(l)$. Let us define $\rho^2_{B,ds} = \frac{1}{N_m}\sum_{l=0}^{\lfloor(N_{os,k}-1)/2^{\eta_k}\rfloor}|F_m(l\cdot 2^{\eta_k})|^2\tilde{\tilde{d}}_i(l\cdot 2^{\eta_k})$. It is easy to get $\rho^2_{B,ds} = \frac{N}{N_m}\frac{1}{2^{\eta_k}}$ and $\rho^2_{B,ot} = \rho_B^2 - \rho^2_{B,ds} = \frac{N}{N_m}[1-\frac{1}{2^{\eta_k}}]$. Similarly, for the m-th subband, we can write $\rho_m^2 = \sum_{i\in\mathcal{U}_m}\frac{1}{N_m}\text{trace}(\mathbf{A}_m\mathbf{d}_i\mathbf{d}_i^H\mathbf{A}_m^H) = \rho^2_{m,ds} + \rho^2_{m,ot}$ with

$\rho^2_{m,ds} = \frac{1}{N_m}\frac{1}{2^{\eta_k}}N_m = \frac{1}{2^{\eta_k}}$. According to the property of the filter, the majority power is at the diagonal elements of $\mathbf{F}_{N_{os,k},m}$ which belong to the m-th subband. Similarly, trace$(\tilde{\mathbf{D}}) = N_m$ and also the majority power is at the same location, which means that the subcarriers which belong to the m-th subband contribute more power to ρ^2_m than others, results in $\rho^2_{m,ot} \geq (N - \frac{N}{2^{\eta_k}})\frac{1}{N}$ and $\rho^2_m = \rho^2_{m,ds} + \rho^2_{m,ot} \geq 1$, i.e., $\frac{1}{\rho^2_m} \geq 1$. i.e., $\overline{SNR}_m \leq \frac{N}{L_{2,max}}\frac{\varrho^2}{\sigma^2} = \overline{SNR}^{ofdm}$.

Appendix C
Proof of Proposition 4

In high-SNR region, average capacity per subcarrier can be approximated as $\overline{C}_m \approx \frac{1}{N_m}$ $\sum_{n\in\mathcal{U}_m}\mathcal{E}(\log_2[SNR(n)])$. Using the SNR expression in (8), we have $\overline{C}_m \approx \frac{1}{N_m}\mathcal{E}\big(\sum_{n\in\mathcal{U}_m}$ $\log_2[\alpha/\rho^2_m|H_k(n,t)|^2|F_m(n)|^2]\big)$ $=$ $\frac{1}{N_m}\mathcal{E}\big(\log_2[(\alpha/\rho^2_m)^{N_m}\Pi_{n\in\mathcal{U}_m}|H_k(n,t)|^2|F_m(n)|^2]\big)$. Since it is assumed that the subband is narrow enough so that the subcarriers lie in the coherence bandwidth, $\overline{C}_m \approx \frac{1}{N_m}\mathcal{E}\big(\log_2[(\alpha/\rho^2_m|H_k(i,t)|^2)^{N_m}|\Pi_{n\in\mathcal{U}_m}F_m(n)|^2]\big)$, where $i \in \mathcal{U}_m$. Using inequality of arithmetic and geometric means [26] (pp20, Chapter 2), we have $|\Pi_{n\in\mathcal{U}_m}F_m(n)|^2 \leq (\frac{1}{N_m}\sum_{n\in\mathcal{U}_m}|F_m(n)|^2)^{N_m}$ $=$ $(\frac{1}{N_m}N_m)^{N_m} = 1$. Then $\overline{C}_m \leq$ $\frac{1}{N_m}\mathcal{E}\big(\log_2[(\alpha/\rho^2_m|H_k(i,t)|^2\frac{1}{N_m})^{N_m}]\big)$ $=$ $\mathcal{E}(\log_2[\alpha/\rho^2_m|H_k(i,t)|^2)]$. As shown in Appendix B, $\rho^2_m \geq 1$, therefore, $\overline{C}_m \leq \mathcal{E}\big(\log_2[\alpha|H_k(i,t)|^2]\big) = C^{ofdm}$.

Appendix D
Proof of Proposition 5

Using (12) and (13), we have $BER(n)$ $=$ $\varpi_1 e^{-\phi_1 SNR(n)} + \varpi_1 e^{-\phi_2 SNR(n)}$, where $\varpi_1 = \frac{1}{6}(1 - \frac{1}{\sqrt{M_{mod}}})$ and $\varpi_2 = \frac{1}{3}(1 - \frac{1}{\sqrt{M_{mod}}})$. Then the average BER in the m-th subband can be given as BER_m $=$ $\frac{1}{N_m}\mathcal{E}\big[\sum_{n\in\mathcal{U}_m}BER(n)\big] = \frac{1}{N_m}\mathcal{E}\big(\varpi_1\sum_{n\in\mathcal{U}_m}e^{-\phi_1 SNR(n)} +$ $\varpi_2\sum_{n\in\mathcal{U}_m}e^{-\phi_2 SNR(n)}\big)$. Let us consider the two expressions one-by-one. Using inequality of arithmetic and geometric means [26] (pp20, Chapter 2), we have $\frac{1}{N_m}\sum_{n\in\mathcal{U}_m}e^{-\phi_1 SNR(n)} \geq (\Pi_{n\in\mathcal{U}_m}e^{-\phi_1 SNR(n)})^{1/N_m} =$ $e^{-\phi_1 1/N_m\sum_{n\in\mathcal{U}_m}SNR_m(n)}$. Using the SINR equation in (8), we obtain $e^{-\phi_1 1/N_m\sum_{n\in\mathcal{U}_m}SNR_m(n)} \approx$ $e^{-\phi_1 1/N_m|H_k(i,t)|^2\sum_{n\in\mathcal{U}_m}\alpha 1/\rho^2_m|F_m(n)|^2}$ $=$ $e^{-\phi_1|H_k(i,t)|^2\alpha 1/\rho^2_m}$. Since both ϕ_1 and N_m are positive values, $\rho^2_m \geq 1$ and according to Proposition 2, it is trivial to obtain $e^{-\phi_1|H_k(i,t)|^2\alpha 1/\rho^2_m} \geq e^{-\phi_1|H_k(i,t)|^2\alpha}$.

References

[1] L. Zhang, A. Ijaz, P. Xiao, and R. Tafazolli, "Multi-service system: An enabler of flexible 5g air interface," *IEEE Communications Magazine*, vol. 55, no. 10, pp. 152–159, OCTOBER 2017.

[2] 5GNOW, "D3.2: 5G waveform candidate selection," Tech. Rep., 2014.

[3] G. Wunder, P. Jung, M. Kasparick, T. Wild, F. Schaich, Y. Chen, S. Brink, I. Gaspar, N. Michailow, A. Festag, L. Mendes, N. Cassiau, D. Ktenas, M. Dryjanski, S. Pietrzyk, B. Eged, P. Vago, and F. Wiedmann, "5GNOW: non-orthogonal, asynchronous waveforms for future mobile applications," *IEEE Communications Magazine*, vol. 52, no. 2, pp. 97–105, February 2014.

[4] V. Vakilian, T. Wild, F. Schaich, S. Ten Brink, and J.-F. Frigon, "Universal-filtered multi-carrier technique for wireless systems beyond LTE," in *IEEE Globecom Workshops (GC Wkshps)*, 2013, pp. 223–228.

[5] X. Chen, S. Zhang, and A. Zhang, "On MIMO-UFMC in the presence of phase noise and antenna mutual coupling," *Radio Science*, vol. 52, no. 11, pp. 1386–1394, 2017.

[6] E. Dahlman, S. Parkvall, and J. Skold, *4G: LTE/LTE-Advanced for Mobile Broadband*. Academic Press, 2011.

[7] D. S. Sesia, M. M. Baker, and M. I. Toufik, *LTE: The UMTS Long Term Evolution: from Theory to Practice*, 2nd ed. Wiley-Blackwell, 2011.

[8] B. Farhang-Boroujeny, "OFDM versus filter bank multicarrier," *IEEE Signal Processing Magazine*, vol. 28, no. 3, pp. 92–112, May 2011.

[9] L. Zhang, P. Xiao, A. Zafar, A. ul Quddus, and R. Tafazolli, "FBMC system: An insight into doubly dispersive channel impact," *IEEE Transactions on Vehicular Technology*, vol. PP, no. 99, pp. 1–14, 2016.

[10] F. Schaich and T. Wild, "Relaxed synchronization support of universal filtered multi-carrier including autonomous timing advance," in *International Symposium on Wireless Communications Systems (ISWCS)*, 2014, pp. 203–208.

[11] A. Farhang, N. Marchetti, F. Figueiredo, and J. P. Miranda, "Massive MIMO and waveform design for 5th generation wireless communication systems," in *International Conference on 5G for Ubiquitous Connectivity (5GU)*, 2014, pp. 70–75.

[12] A. Ijaz *et al.*, "Enabling massive IoT in 5G and beyond systems: PHY radio frame design considerations," *IEEE Access*, vol. 4, pp. 3322–3339, 2016.

[13] X. Wang, T. Wild, F. Schaich, and A. Fonseca dos Santos, "Universal filtered multi-carrier with leakage-based filter optimization," in *European Wireless Conference*, 2014, pp. 1–5.

[14] W. Xiaojie, W. T, S. F, and B. S. ten, "Pilot-aided channel estimation for universal filtered multi-carrier," in *IEEE Vehicular Technology Conference (VTC Fall)*, 2015.

[15] X. Yu, T. Wild, and F. Schaich, "Impact of RF transmitter hardware on 5G waveforms: Signal conditionings for UF-OFDM," in *International Symposium on Wireless Communication Systems (ISWCS)*, 2016, pp. 153–157.

[16] Y. Chen, F. Schaich, and T. Wild, "Multiple access and waveforms for 5G: IDMA and universal filtered multi-carrier," in *IEEE Vehicular Technology Conference (VTC Spring)*, 2014, pp. 1–5.

[17] L. Zhang, P. Xiao, and A. Quddus, "Cyclic prefix-based universal filtered multicarrier system and performance analysis," *IEEE Signal Processing Letters*, vol. 23, no. 9, pp. 1197–1201, Sept 2016.

[18] H. Steendam and M. Moeneclaey, "Analysis and optimization of the performance of OFDM on frequency-selective time-selective fading channels," *IEEE Transactions on Communications*, vol. 47, no. 12, pp. 1811–1819, 1999.

[19] Y. Huang and B. D. Rao, "Awareness of channel statistics for slow cyclic prefix adaptation in an OFDMA system," *IEEE Wireless Communications Letters*, vol. 1, no. 4, pp. 332–335, 2012.

[20] X. Wang, T. Wild, and F. Schaich, "Filter optimization for carrier-frequency-and timing-offset in universal filtered multi-carrier systems," in *IEEE Vehicular Technology Conference (VTC Spring)*, 2015, pp. 1–6.

[21] L. Zhang, A. Ijaz, P. Xiao, A. Quddus, and R. Tafazolli, "Subband filtered multi-carrier systems for multi-service wireless communications," *IEEE Transactions on Wireless Communications*, vol. 16, no. 3, pp. 1893–1907, March 2017.

[22] T. Van Waterschoot, V. Le Nir, J. Duplicy, and M. Moonen, "Analytical expressions for the power spectral density of CP-OFDM and ZP-OFDM signals," *IEEE Signal Processing Letters*, vol. 17, no. 4, pp. 371–374, 2010.

[23] D. Chen, X.-G. Xia, T. Jiang, and X. Gao, "Properties and power spectral densities of CP based OQAM-OFDM systems," *IEEE Transactions on Signal Processing*, vol. 63, no. 14, pp. 3561–3575, 2015.

[24] B. Muquet, Z. Wang, G. B. Giannakis, M. De Courville, and P. Duhamel, "Cyclic prefixing or zero padding for wireless multicarrier transmissions?" *Communications, IEEE Transactions on*, vol. 50, no. 12, pp. 2136–2148, 2002.

[25] N. Kim, Y. Lee, and H. Park, "Performance analysis of MIMO system with linear MMSE receiver," *IEEE Transactions on Wireless Communications*, vol. 7, no. 11, pp. 4474–4478, 2008.

[26] J. M. Steels, *The Cauchy-Schwarz Master Class: An Introduction to the Art of Mathematical Inequalities*. Cambridge University Press, 2004.